

Characterization of biodegradable polymers: A review

Abolade Shuqrat Busari *

Department Of Chemistry and Biochemistry, Central Michigan University, Michigan, USA.

World Journal of Advanced Research and Reviews, 2024, 23(01), 3153-3161

Publication history: Received on 25 May 2024; revised on 23 July 2024; accepted on 26 July 2024

Article DOI: <https://doi.org/10.30574/wjarr.2024.23.1.2018>

Abstract

The growing concern over global pollution, particularly from non-degradable plastics, has driven the search for sustainable alternatives. Biodegradable polymers offer a promising solution by combining functionality with environmental compatibility. This review focuses on the characterization of three key biodegradable polymers polycaprolactone (PCL), polylactic acid (PLA), and polybutylene succinate (PBS), highlighting their structural, thermal, and morphological properties. Techniques such as Fourier Transform Infrared Spectroscopy (FTIR), Nuclear Magnetic Resonance (NMR), Scanning Electron Microscopy (SEM), and Differential Scanning Calorimetry (DSC) are employed to analyze these polymers, revealing insights into their molecular structure, crystallinity, biocompatibility, and thermal behavior. The findings underscore the potential of PCL, PLA, and PBS in diverse applications, from biomedical engineering to packaging, while addressing the urgent need for materials that mitigate environmental impact. This paper consolidates current knowledge to advance the development and optimization of biodegradable polymers for a sustainable future.

Keywords: Biodegradable Polymers; Environmental Pollution; Polycaprolactone; Polylactic Acid; Polybutylene Succinate

1. Introduction

For many years there has been a primary concern over global pollution and how it affects the planet [1]. Therefore, it is of utmost importance to find alternatives to substitute materials and processes to develop a more sustainable society. Among the many issues of world pollution, plastics are pointed to as one of the main problems due to their incorrect disposal, ending in land, air, or water [2–4]. Since the modern era, it seems nearly impossible to have a society without plastics [5]. Therefore, tackling pollution problems with as many solutions as possible with the most negligible impact on the coevolution of materials and society is crucial. Biodegradable polymers are viable alternatives to nondegradable plastics for the abatement of environmental pollution. IUPAC defines biodegradable polymers as “polymer susceptible to degradation by biological activity, with the degradation accompanied by a lowering of its molar mass” [1]. These are generally polymers with hydrolysable backbones, esters, amides, and urethanes. Biodegradation occurs either by hydrolysis or oxidative mechanisms. In the initial stage, the polymers are broken down into smaller fragments, resulting in a reduction in the molecular mass.

In this review paper, three biodegradable polymers are going to be the focus.

1.1. Polycaprolactone (PCL)

Polycaprolactone is a semicrystalline linear polyester produced by ring-opening polymerization of *epsilon*-caprolactone, which is commonly derived from fossil carbon. It has a much lower glass-transition temperature ($T_g = -60\text{ }^\circ\text{C}$) than other biodegradable polymers which assist its biodegradability despite its high degree of

* Corresponding author: Abolade Shuqrat Busari

crystallinity, typically 50%. The melting point ($T_m = 60\text{ }^\circ\text{C}$) is also rather low. Like poly(butylene succinate) (PBS), PCL is often used in biodegradable polymer blends such as PCL/PHB (Lovera *et al.*, 2007), PCL/starch (Averous *et al.*, 2000) and PCL/PLA (Liu *et al.*, 2000).

1.2. Poly lactic acid (PLA)

Poly (lactic acid), Fig. 13.1, is an aliphatic ester of the poly(2-hydroxy) type, the most significant other example of which is poly (glycolic acid) (PGA). Although these two polymers were discovered in the mid-1950s, they were initially disregarded on account of their hydrothermal instability, which prevented their use in the injection moulding and extrusion processes. In the 1960s, the first use of PGA to make dissolving artificial sutures was reported (Schmitt and Polistina, 1969). In this application, sensitivity to water was an advantage and thus PGA provided the first practical alternative to denatured collagen. This property of in vivo degradability was also demonstrated for poly (L-lactic acid) and poly (DL lactic acid) (Kulkarni *et al.*, 1966).

1.3. Poly butylene succinate (PBS)

Of the synthetic biodegradable polymers available, poly (butylene succinate), has attracted much attention because it is comparable with poly(propylene) in terms of good thermal resistance and melt processability as well as its chemical resistance, whilst remaining biodegradable (Ray *et al.*, 2005). Although it was originally derived from fossil carbon, there is considerable interest in developing it as a bio-sourced polymer, with the succinic acid moiety being produced by bacteria such as *E. coli* or commercially developed strains such as *Basfi succiniproducens* from glucose or glycerol feedstock. PBS is suitable for film forming, sheet extrusion, injection molding and molded foam products.

2. Characterization of the polymers

2.1. Fourier Transform Infra-Red Spectroscopy (FTIR for PCL)

From FTIR spectrum of the chosen polycaprolactone (Figure 1), the absorption band at 2940 cm^{-1} is assigned to the C-H hydroxyl groups asymmetric stretching. The band at 2860 cm^{-1} is assigned to C-H hydroxyl groups symmetric stretching. The absorption band at 1722 cm^{-1} is assigned to C=O stretching vibrations of the ester carbonyl group. The absorption at 1238 cm^{-1} is assigned to C-O-C asymmetric stretching, but the signal at 1160 cm^{-1} is assigned to C-O-C symmetric stretching. [6]

2.2. Nuclear Magnetic Resonance (NMR for PCL)

NMR spectrum of synthesized PCL is given in Fig 2. This spectrum clearly indicates that properties of the synthesized polymer were consistent with the data of PCL. Chemical shifts (ppm) of PCL seen can be described as: 4.1 ppm (ethyl group on the oxygen side of the ester bond), 3.9–4.0 ppm (α -helical structure, assigned to the protons of CH_2), 3.56–3.59 ppm (the presence of hydroxymethyl end group (CH_2OH)), 2.56–2.59 ppm (3CH_3), 2.3 ppm (CH_2CO), 1.5–1.7 ppm (2CH_2), 1.3 ppm (CH_2 which indicates that structure of the PCL polymer still remains). This molecular structure is specific to PCL and is also consistent with what is reported in literature [6]

2.3. Scanning Electron Microscopy (SEM for PCL)

Biocompatibility of the PCL was partially probed by examining the attachment and response of the mesenchymal stem cells. Attachment of the cells to the fibers was evident within 72 h of seeding. Observations demonstrated that synthesized PCL scaffold is suitable for mesenchymal stem cell attachment and survival. PCL scaffolds were previously shown to support the attachment, survival, and activity of mesenchymal stem cells derived from bone marrow [7], as well as adipose tissues.

2.4. Differential Scanning Calorimetry (DSC for PCL)

DSC graph of the PCL alone shows the melting point at $59.3\text{ }^\circ\text{C}$, whereas the graph of gelatin (GN) manifests a very wide endothermic peak, most likely due to water evaporation during the thermal scanning. The peak related to water evaporation is present also for the coaxial and blend systems, whereas it is absent for the PCL alone, confirming that water absorption is due to the high GN hydrophilicity, suggesting, as expected, that the more is the GN quantity, the wider and more relevant is the peak (between 50 and $100\text{ }^\circ\text{C}$) after the main melting point of PCL. On the one hand, the PCL melting peak is slightly anticipated from $59.3\text{ }^\circ\text{C}$ for the pure PCL to $58\text{ }^\circ\text{C}$ for both the coaxial systems, whereas the blend systems show higher anticipation of the melting point according to the GN amount. The anticipation of the melting point suggests the formation of smaller crystallites that requires lower temperature energy to melt [8].

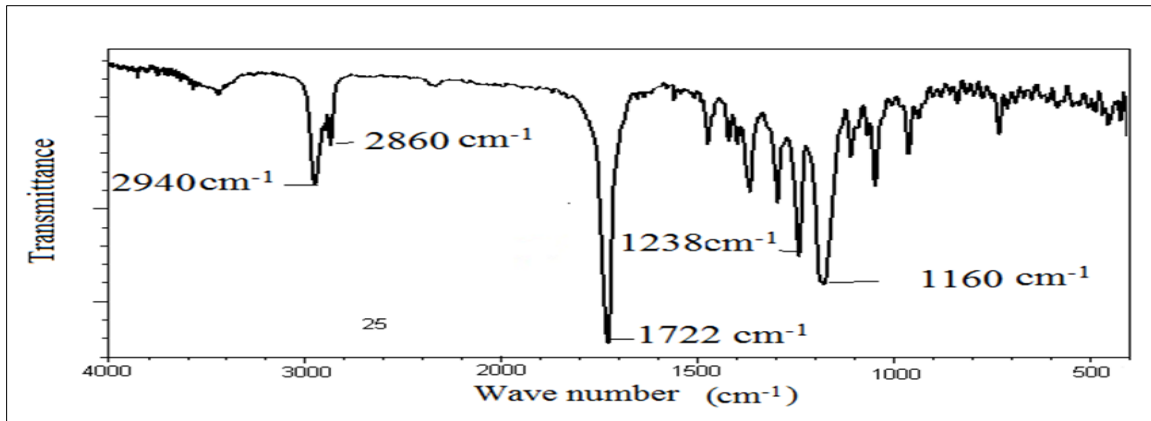


Figure 1 FTIR spectra of PCL

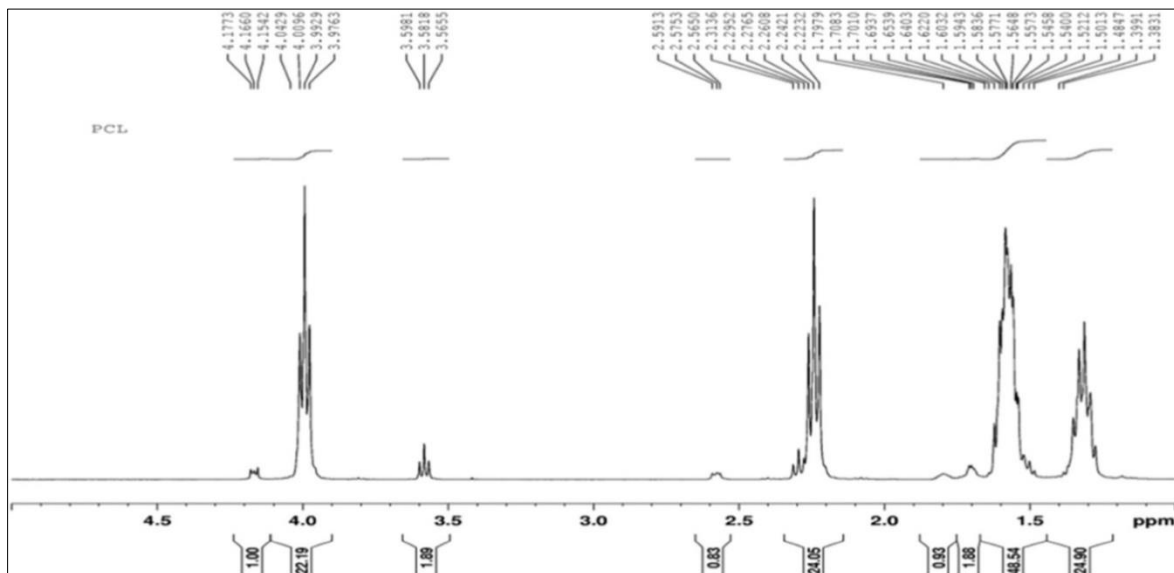


Figure 2 NMR spectra of PCL

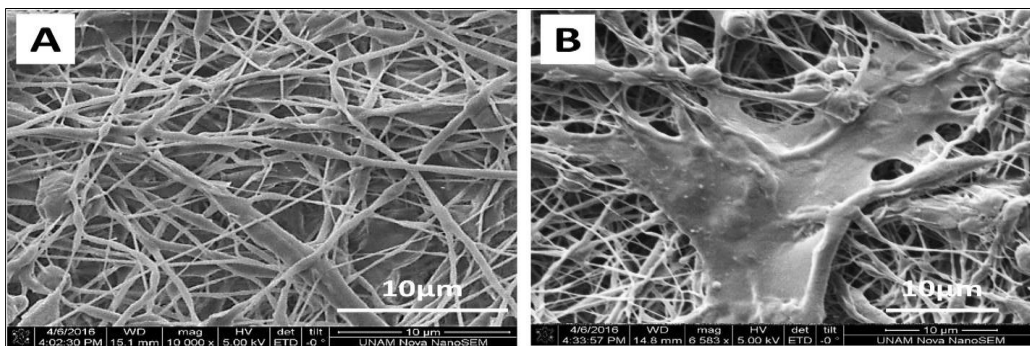


Figure 3 SEM micrographs of scaffolds produced from synthesized PCL. (A) Cell free, and (B) cellularized scaffolds

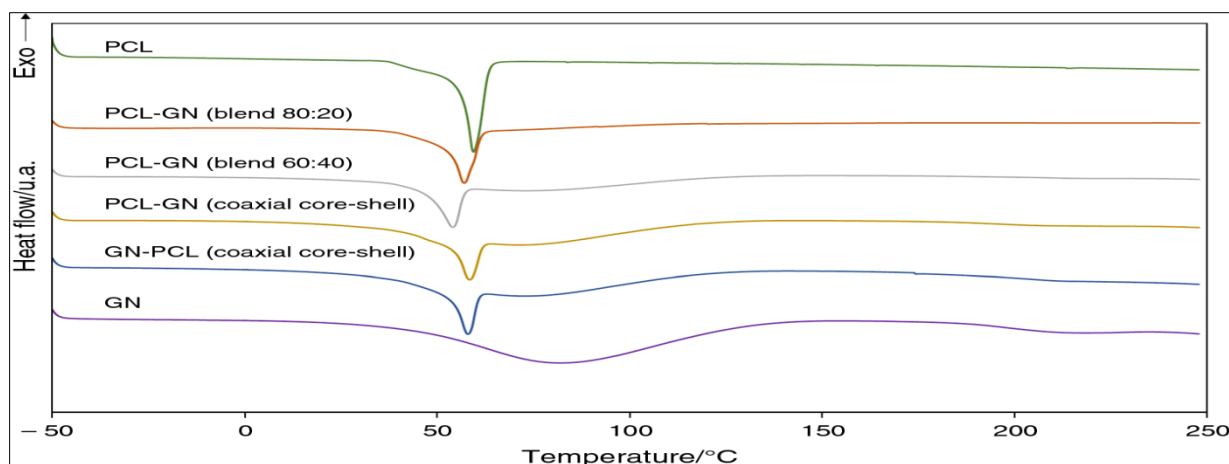


Figure 4 DSC OF PCL and PCL-GN blends

2.5. Fourier Transform Infra-Red Spectroscopy (FTIR for PLA)

The spectrum of PLA shows characteristic peaks at around 1100, 1450 and 1750 cm^{-1} , which are attributed to vibrational bands of C–O–C, C–H bonds and C=O stretching of esteric groups on PLA chains. Peaks around 2980–3000 cm^{-1} indicate the stretching vibrations of aliphatic C–H bonds. Also, displayed peaks at around 1438 and 1556 cm^{-1} corresponding to the C=C stretching of the quinoid ring, and C=C stretching vibration of the benzenoid ring. Peak at around 3400 cm^{-1} prove the vibrations of N–H in polyaniline groups demonstrates the formation of PANI segment in final polymeric structure.[9]

2.6. Nuclear Magnetic Resonance (NMR for PLA)

Figure 4 showed $^1\text{H-NMR}$ spectrum of PLA obtained at 160 °C for 48 h (for Table 1, Entry 3). The spectrum revealed the signal of methane proton resonances in the main chain at 5.15 ppm and the signal of methyl proton resonances in the main chain at 1.57 ppm. A very weak signal about 4.30 ppm and 1.4 ppm assigned to the methine proton and methyl proton next to the terminal hydroxyl group and carboxyl group, respectively. The above results confirmed that poly (lactic acid) was formed.

2.7. Scanning Electron Microscopy (SEM for PLA)

As illustrated in Fig7, the surface morphologies of the PLA scaffolds prepared by selective enzymatic degradation were observed by SEM. The SEM micrographs of the blends after 15 days of degradation and the remaining PLA scaffolds showed that various pores were distributed evenly onto the surface of the PLA scaffolds. However, the morphology and distribution of the pores significantly differed with the change of the composition of P(3HB-co-4HB) in the blends. Through these results we could conclude that polymer composition and degradation time would significantly influence the porous characterizations of the PLA scaffolds *via* selective enzymatic degradation. [10]

2.8. Differential Scanning Calorimetry (DSC for PLA)

The DSC thermogram of PLA shows two peaks. The first endothermic peak was attributed to cold crystallization of PLA at 136.8 °C and the second exothermic peak was regarded to decomposition of the PLA. The DSC thermogram of copolymer (blue one) shows three peaks. The first peak is related to the removal of water and other solvents. The second peak at 324 °C same as the second peak in PLA diagram is regarded to decomposition of PLA part in copolymer. The peak at 552 °C is attributed to decomposition of PANI segment part in copolymer. [11]

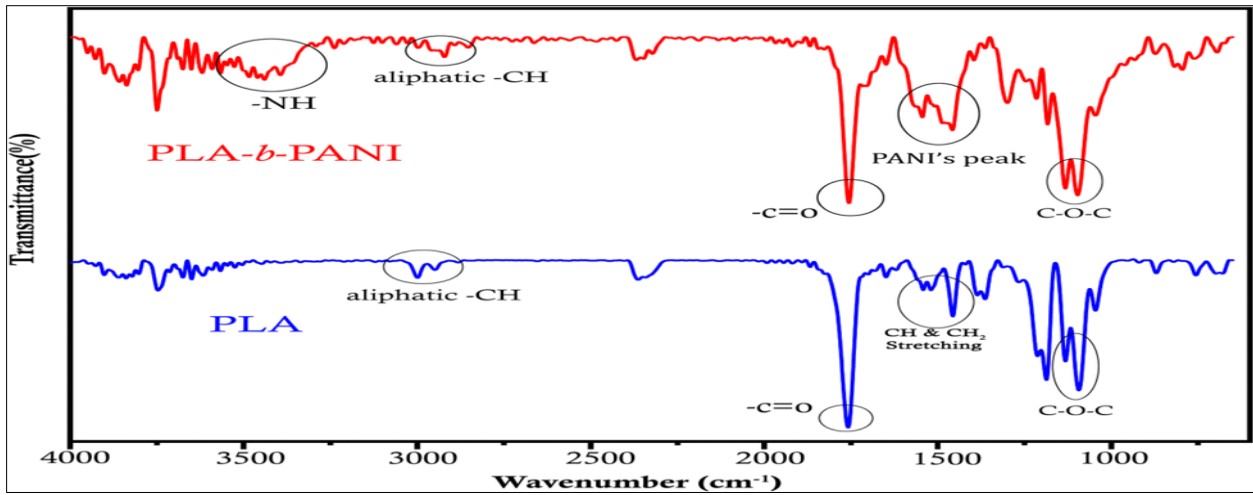


Figure 5 FT-IR spectra of PLA and PLA-b-PANI

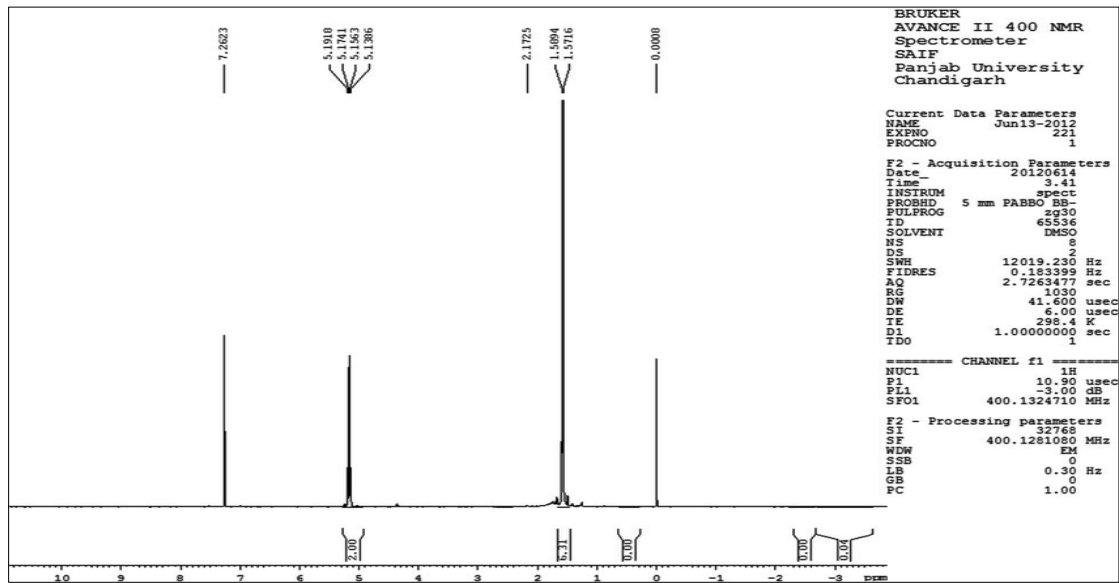


Figure 6 NMR spectra of PLA

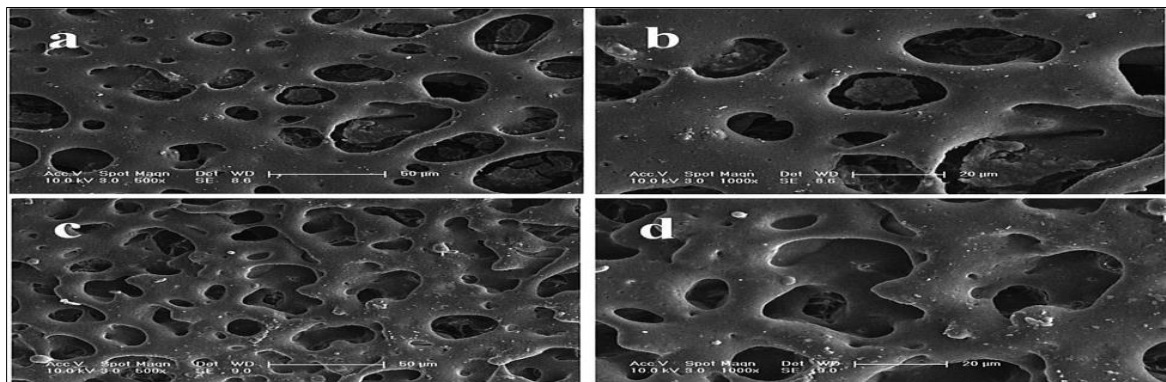


Figure 7 SEM images of PLA/P(3HB-co-4HB) blends (wt/wt, 50/50) after different degradation times: 15 days of degradation (a, b), 30 days of degradation (c, d)

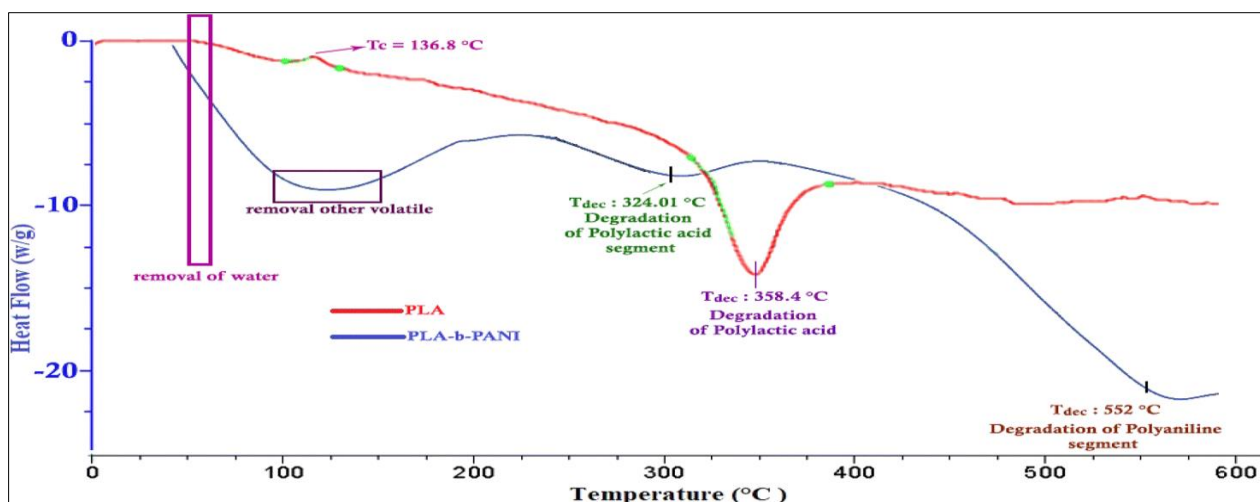


Figure 8 DSC analysis for PLA (red diagram) and PLA-*b*-PANI (blue diagram)

2.9. Fourier Transform Infra-Red Spectroscopy (FTIR for PBS)

The FTIR spectrum of Polybutylene succinate presented in Figure 9 shows an absorption band at 2947 cm^{-1} assigned to the C-H bond stretching. The band intense appeared at 1716 cm^{-1} corresponds to carbonyl C=O stretching vibration characterizing the formation of ester group. Furthermore, the peak present at 1341 cm^{-1} is assigned to -COO- bond stretching vibration. The signal at 1158 cm^{-1} is a characteristic of C-O-C stretching vibration in the repeated -OCH₂CH₂ unit. These vibration bands described that the polycondensation reaction was successful.

2.10. Nuclear Magnetic Resonance (NMR for PBS)

¹H-NMR spectra were obtained to compare with the literature and prove the pristine composition. As we can see in figure 10, the spectra of PBAT, PBS, and PHBV confirmed the chemical structure of each polymer by the presence of characteristic protons PBS CH₂ proton signals appear at 4.11, 2.62, and 1.7 ppm as indicated and confirmed in literature [13, 14].

2.11. Scanning Electron Microscopy (SEM for PBS)

PBS exhibits a semi-ductile fracture behavior, indicated by the relatively smooth and clear surface with fibrils that formed a web-like structure. In Figure 11b, fractured surface of PBS/ 2%OMMT nanocomposites reveals a reduction in the fibrillation of PBS, due to the stiffening effect after OMMT addition. The formation of microcavities at the filler-matrix interface is caused by the poor compatibility between PBS and OMMT, which is the main reason for the limited properties enhancement.

2.12. Differential Scanning Calorimetry (DSC for PBS)

The thermal behavior of PBS nanocomposites is studied from the DSC analysis and reported in Figure 12. Figure 12a shows two distinct peaks in the heating scans of PBS and its nanocomposites. Similar observation has been reported by Ray et al. [12] and Vega-Baudrit et al. [13], where they pointed out the existence of two melting peaks was due to the two different types of crystalline lamella presented in PBS. They suggested that the lower melting endotherm corresponds to the melting of the original crystallites formed at the isothermal crystallization temperature, while the higher melting endotherm reveals the melting of the recrystallized crystal.

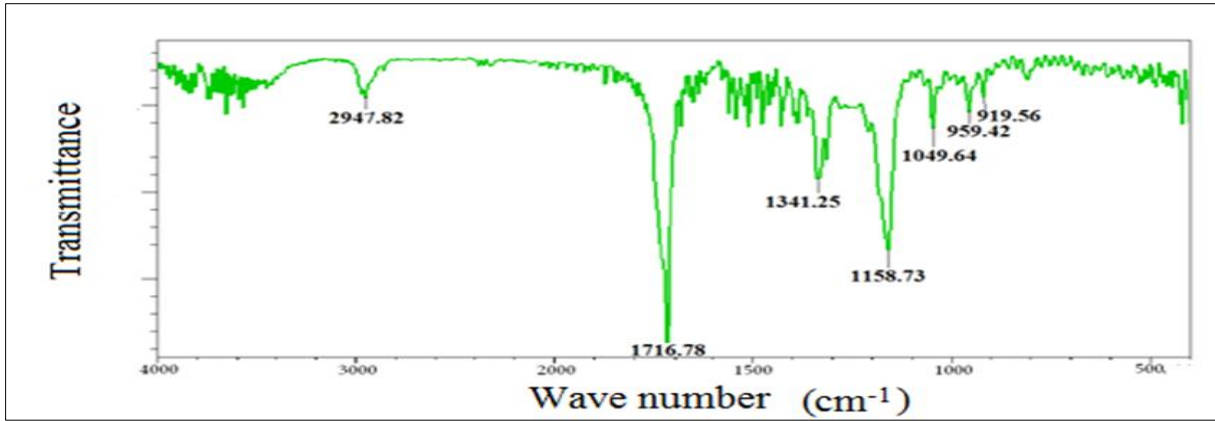


Figure 9 FTIR spectra of PBS

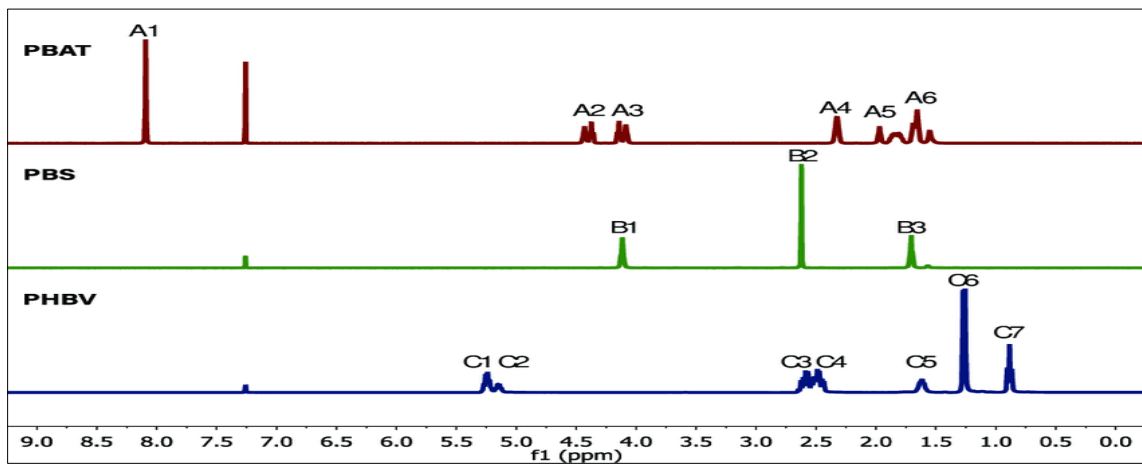


Figure 10 ¹H-NMR spectra of PBAT, PBS, and PHBV

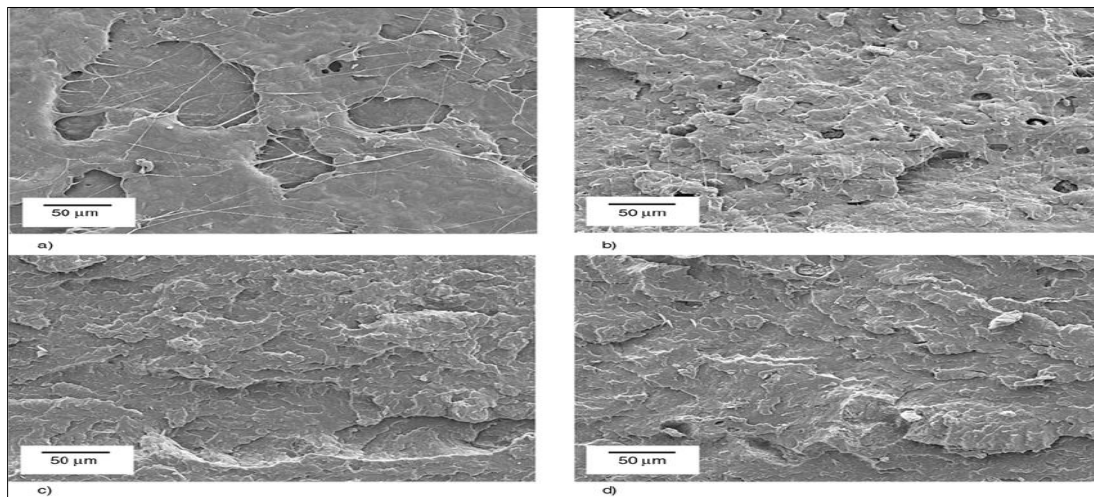


Figure 11 The tensile fractured surface of PBS and its nanocomposites

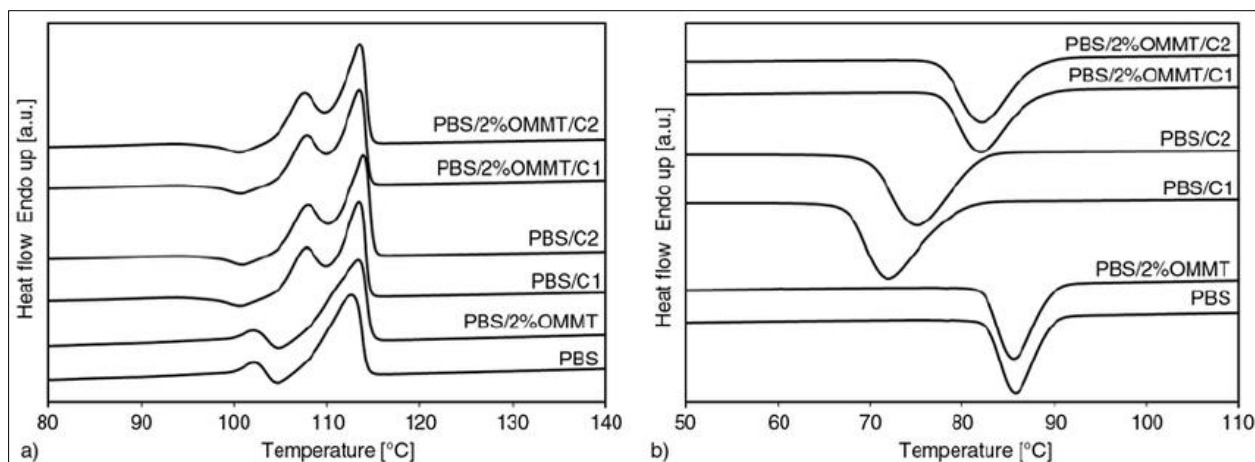


Figure 12 DSC Analysis for PBS and PBS blends

3. Conclusion

As PCL and PLA are both synthesized by ring-opening polymerization, PCL/PLA multiblock copolymers can readily be produced, to give biodegradable thermoplastic elastomers (Cohn and Hotovely Salomon, 2005). PLA/GA copolymers are widely used in biomedical applications because of their biocompatibility and range of properties obtainable by manipulation of the formulation conditions. Lactic acid, unlike glycolic acid, contains an asymmetric carbon atom and therefore has two optically active enantiomers, D and L. Lactic acid readily forms cyclic esters, or lactides, composed of two lactic acid units or dimers.

The range of applications for which PBS is currently marketed include mulching film, compost bags and household goods. It is also used in some civil engineering and construction applications. It has good fibre-forming properties and is therefore suitable for spun-fibre applications such as textiles. PBS is often blended with other polymers to give materials with improved properties such as impact strength. Examples of PBS blends with other biodegradable polymers include PBS/PLA (Chen et al., 2005; Harada et al., 2007; Park and Im, 2002) and PBS/PHA (Qiu et al., 2003)

References

- [1] Fuller, R. et al., Pollution and health: a progress update. *The Lancet Planetary Health* 6(6), 535–547 (2022). [https://doi.org/10.1016/S2542-5196\(22\)00090-0](https://doi.org/10.1016/S2542-5196(22)00090-0)
- [2] Villarrubia-Gómez, P. et al., Marine plastic pollution as a planetary boundary threat – the drifting piece in the sustainability puzzle. *Marine Policy* 96, 213–220 (2018). <https://doi.org/10.1016/j.marpol.2017.11.035>
- [3] de Souza Machado, et al., Microplastics as an emerging threat to terrestrial ecosystems. *Global Change Biology* 24(4), 1405–1416 (2018) <https://arxiv.org/abs/https://onlinelibrary.wiley.com/doi/pdf/10.1111/gcb.14020>.
- [4] Agathokleous, E. et al., Ecological risks in a ‘plastic’ world: A threat to biological diversity? *Journal of Hazardous Materials* 417, 126035 (2021). <https://doi.org/10.1016/j.jhazmat.2021.126035>
- [5] Evans, D.M. et al., Understanding plastic packaging: The co-evolution of materials and society. *Global Environmental Change* 65, 102166 (2020). <https://doi.org/10.1016/j.gloenvcha.2020.102166>
- [6] Michael F. Ashby, in *Materials and the Environment* (Second Edition), 2013
- [7] P.P. Lui Stem cell technology for tendon regeneration: current status, challenges, and future research directions *Stem Cells Cloning*, 8 (2015), pp. 163-174
- [8] Longo, R., Catauro, M., Sorrentino, A. et al. Thermal and mechanical characterization of complex electrospun systems based on polycaprolactone and gelatin. *J Therm Anal Calorim* 147, 5391–5399 (2022). <https://doi.org/10.1007/s10973-022-11225-7>
- [9] Suprakas Sinha Ray, et al., Sustainable Poly lactide-Based Blends 2022 <https://doi.org/10.1016/B978-0-323-85868-7.00017-2>

- [10] M. Trchová and J. Stejskal, Polyaniline: The infrared spectroscopy of conducting polymer nanotubes (IUPAC Technical Report), *Pure Appl. Chem.*, 2011, 83, 1803–1817 CrossRef.
- [11] N. Bagheri, M. M. Lakouraj, V. Hasantabar and M. Mohseni, Biodegradable macro-porous CMC-polyaniline hydrogel: Synthesis, characterization and study of microbial elimination and sorption capacity of dyes from wastewater, *J. Hazard. Mater.*, 2021, 403, 123631 CrossRef CAS PubMed.
- [12] Nifant'ev, I.E., Bagrov, V.V., Komarov, P.D., Ilyin, S.O., Ivchenko, P.V.: The use of branching agents in the synthesis of pbat. *Polymers* 14(9) (2022). <https://doi.org/10.3390/polym14091720>
- [13] Zhou, X., Wu, T.: Synthesis, characterization of phosphorus-containing copolyester and its application as flame retardants for poly (butylene succinate) (pbs). *Chemosphere* 235, 163–168 (2019). <https://doi.org/10.1016/j.chemosphere.2019.06.151>
- [14] Zhang, Y. et al., Synthesis, physical properties and photodegradation of functional poly (butylene succinate) covalently linking uv stabilizing moieties in molecular chains. *Colloids and Surfaces A: Physicochemical and Engineering Aspects* 524, 160–168 (2017). <https://doi.org/10.1016/j.colsurfa.2017.04.025>